

Performance of SVM technique for DoA Estimation in 5G mm-Wave band

DOI:10.36909/jer.12013

Youmni Ziade*, Wissam Obeid**

*Electrical and Computer Engineering Department, Beirut Arab University, Tripoli, Lebanon.

** Laboratory of Signals and Systems (L2S), CentraleSupélec, Gif-sur-Yvette, France.

* Corresponding Author: y.ziadeh@bau.edu.lb

ABSTRACT

Applying Machine Learning algorithms in wireless communication has shown increasing interest due to the increase of demand on capacity, the increase of the number of users, and equipment sharing the limited frequency spectrum resources. Also, the need for a reduction in power consumption at base stations and the optimization of radio coverage make ML an attractive and promising technique. In this paper, we investigate the usage of Support Vector Machine (SVM) technique for Direction of Arrival (DoA) estimation in the millimeter-wave band. The objective is to predict the location of a user in a given area by analyzing the received signals at an array of antennas, using an SVM-based model. The first phase of this technique consists of the training phase that aims to identify the characteristics of each class, and that is based on a set of training samples. The second phase consists of testing the trained model using a set of samples/users. We have carried out a set of simulations based on the developed model. The results are promising in terms of the accuracy of determining the DoA, taking into consideration a channel with noise and multipath.

Keywords: Machine learning, SVM, DoA, mm-Wave, Beamforming.

INTRODUCTION

High data rates, large number of users, low latency, high reliability, and low energy consumption are the major performance requirements of the next generation of wireless networks. One of the main constraints that will be encountered to fulfill these requirements is the limited and crowded spectrum. Thus, the challenge will be in investigating new frequency bands and in assisting and managing the available frequency bands in an intelligent, optimized, and adaptive manner (Yarrabothu & Mohan, 2015; Chin et al., 2014). Relying on the existing technologies used in the actual wireless networks is not sufficient and new tools and techniques are to be proposed, developed, and applied.

Exploring new frequency bands is crucial due to two main factors: the saturation of the existing spectra and the increasing data rates and numbers of users in the new generation networks. The millimeter-wave (mm-wave) band seems to be a promising candidate for the radio access in urban and crowded areas and for small cells coverage, thanks to new technologies that have enabled to design transceivers of good performance at this band (Niu et al., 2015; Heath et al., 2016; Al-Falahy et al., 2019; Cella et al., 2014). Mm-wave band shows high propagation loss, due to free space propagation loss given by FRIIS equation (Equation 1), atmospheric absorption, and blockage from buildings and other obstacles (Rappaport et al., 2017). Although this characteristic constitutes an issue in decreasing the coverage range, it allows the frequency reuse and the reduction of interference at close cells and is convenient for small cells design.

$$FSL(dB) = 32.44 + 20\log(f_{MHz}) + 20\log(D_{km}) \quad (1)$$

These new bands are to be used in conjunction with other technologies as cognitive radio (CR) network (Liang et al., 2011, Liu et al., 2017), heterogeneous networks (Bogale & Le, 2016; Bshara et al., 2018) following an intelligent, dynamic, and adaptive algorithms.

The information about the user location within a cell is essential for optimum beneficial use of these new technologies. The aim in the context of our work is to find, define, and implement a smart model to detect the position of a specific user in a cell and evaluate its performance in a realistic configuration. Based on this model results, a beamforming can be performed afterwards to direct the electromagnetic radiation of the antenna array towards the regions of concentration of users. The flowchart of the proposed implementation of the trained model in a realistic application is shown in Figure 1.

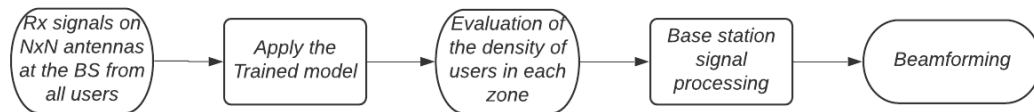


Figure 1 - Proposed implementation.

Many methods have been proposed for DoA estimation. One of the most popular methods is the multiple signal classification algorithm (MUSIC) (Schmidt, 1986). Other methods are proposed as well like the estimation of signal parameters via rotational invariance technique (ESPRIT) (Roy et al., 1989), the maximum likelihood, and stochastic methods based on machine learning and neural networks (Zooghy et al., 1997, Zooghy et al., 2000, Randazzo et al., 2007).

In this paper, we study the localization of a user within a cell by estimating the direction of arrival (DoA) at the base station. The DoA is estimated using an SVM-based algorithm that consists of two main phases: a training phase and a testing phase. In the training phase, the

model is developed based on a set of training samples. The testing phase allows to estimate the position of new samples (users) and to study the accuracy of the developed model and its robustness in the presence of noise and multipaths.

This paper is organized as follows: In the next section, we give an overview of the SVM method and its applications. In section III, we give details of the proposed system and procedure used to predict the location of a user within a cell. In section IV, we analyze the performance of the system by giving and discussing the results of the simulation. We conclude on this work and propose perspectives for further research in section V.

OVERVIEW ON SVM TECHNIQUE AND APPLICATIONS

The Support vector machine technique (SVM) is a supervised machine learning algorithm mainly used to classify a set of numerical data into different classes based on their mathematical properties and characteristics. The classification aims to find the borders between the different classes with the constraint of maximizing the distance from the samples to these borders (or, equivalently, minimizing the error in classification). We note here that the border is a line if the set of data is characterized by two parameters, and it is a plane if three parameters are needed to characterize the data and a hyperplane for a higher number of parameters (Cortes & Vapnik, 1995).

We distinguish between linear and non-linear classification: linear classification refers to the case where the borders between the different classes constitute on hyperplanes (e.g., straight lines in a 2D problem), whereas non-linear classification refers to the case where the borders consist of hypersurfaces (e.g., curved lines in a 2D problem) (Ladicky & Torr, 2011; Suykens, 2001).

The power of SVM originates from the fact that it can be applied for non-linear problems using the Kernel trick which is a phase of data processing prior to SVM classification. This latter, ψ , is a function that transforms numerical data from a low dimensional space into a higher dimensional space where data can be linearly separated into classes (Awad & Khanna, 2015). We start by considering a classification of L samples in \mathbb{R}^d : $S = (x_1, y_1, \dots, x_L, y_L, \dots, x_L, y_L)$ with x_l being the input and y_l being the corresponding label. Consider \mathcal{F} a Hilbert space, and ψ the mapping $\mathcal{X} \rightarrow \mathcal{F}$. It is possible to consider $S^\psi = (\psi(x_1), y_1, \dots, \psi(x_L), y_L)$ where S may not be linearly separable and S^ψ becomes linearly separable if ψ is well chosen. Given a linear classifier w in \mathcal{F} , the predictions are done by $y = \langle \psi(x), w \rangle$.

Once the model is generated based on training data, it is used to analyze new data and predict their classes. The SVM technique has proved a good performance in telecom applications. In Wang et al. (2014), the SVM method is used in CR networks to predict the spectrum mobility in time domain and space domain. Path loss and coverage estimation for different frequency bands

are investigated in many works using machine learning-based techniques and promising results in filling the lack of data are obtained (Zhao et al., 2013; Uccellari et al., 2018; Zhang et al., 2019-1). In Feng et al. (2013) and Xu et al. (2020), SVM is used to classify and identify interference and abnormal signals and the prediction phase has shown good accuracy results. Furthermore, SVM has proved its high efficiency in the estimation of direction of arrivals compared to the conventional methods as Multiple Signal Classification (MUSIC) and Esprit (Randazo et al., 2007). In Sun et al. (2019), a comparison of performance for different Kernel functions for 1-D DoA estimation in the presence of white Gaussian noise is performed.

SYSTEM DESCRIPTION, CONSTRAINTS AND MODEL

We present in this section a comprehensive description of the proposed system for the estimation of user location within a given area. First, we give the geometrical description and configuration of the considered scenarios. Also, we define the system constraints. In the system model part, we detail channel propagation model and the SVM-based method used for classification.

A. System description

The geometrical description of the system is shown in **Error! Reference source not found.**. The base station (BS), located at the border of a cell at a height H , consists of a 2-D antenna array of $N \times N$ elements with a separating distance d . The covered cell has an area of $D \times D$ and is divided into $M \times M$ zones. The size of each zone is $w \times w$. The frequency of operation of the system is f . L is the number of users in each zone. We analyze the estimation of the position of one user within a given cell. When more than one user exists in a cell, each signal from a user is identified and analyzed separately in order to predict its position (Zhang et al., 2019-2).

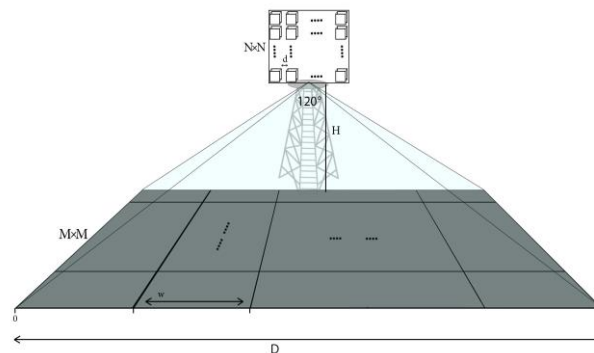


Figure 2 The considered geometrical configuration.

B. System constraints

Various constraints are considered in the definition and the modeling of the system. First, the system should support different numbers of antennas and zones. Second, it will be

applied to 5G mm-wave band, but it should be applicable to any frequency band. Third, the channel of propagation between the BS and users is considered to be time-invariant, should take into account the direct path, the multi-path components, and the noise effects, and should provide information about the magnitude and phase of the received signal at BS.

C. System Model

The system model that we will use to estimate the DoA of a user includes two main parts: the propagation model used to estimate the received signal, and the SVM-based model used to generate the trained model and to predict the location of a new user.

The transmitted narrow-band signal $p(t)$ is a Gaussian pulse given by:

$$p(t) = A \cdot \exp\left(-\frac{(t - t_0)^2}{\sigma^2}\right) \cdot \sin(2\pi f_c(t - t_0)) \quad (2)$$

Where A is the amplitude, f_c the carrier frequency, t_0 a constant that ensures the causality of the pulse, and $\sigma = 3/(8\Delta f)$ with Δf is the bandwidth of the pulse.

The propagation channel is considered to have K multipaths resulting of different phenomena: direct path, reflection, diffraction, transmission, and scattering (Rappaport, 2001; Godara, 2002). The channel impulse response between a user u and an element (i, j) can be written as:

$$h_{i,j}^u(t) = \sum_{k=1}^K \alpha_{i,j}^{u,k} \delta(t - \tau_{i,j}^{u,k}) \quad (3)$$

Where $\tau_{i,j}^{u,k}$ is the time delay of the path k between the user u and the element (i, j) of the array, $\alpha_{i,j}^{u,k}$ is a factor that counts for the total attenuation of the path k between the user u and the array element (i, j) and is inversely proportional to the propagation distance.

The corresponding signal $s_{i,j}^u(t)$ at the receiver is written as given in (Equation 4), with $n(t)$ is an additive white Gaussian noise at the receiver.

$$s_{i,j}^u(t) = h_{i,j}^u(t) * p(t) + n(t) = \sum_{k=1}^K \alpha_{i,j}^{u,k} p(t - \tau_{i,j}^{u,k}) + n(t) \quad (4)$$

The SVM-based model is divided into two main phases: the training phase and the prediction phase. **Error! Reference source not found.** shows the block diagram of the training phase. L users are randomly generated in each of the $M \times M$ considered zones. The users positions coordinates vectors $[X]$ and $[Y]$ (of length $L \times M \times M$ each) are considered to be known. The

received signals from each user over $N \times N$ antennas are then calculated using equation 4 (the noise is not considered in this phase). Thus the resultant matrix $[S]$ of dimension $(L \times M \times M, N \times N)$ is formed. $[S]$ matrix and the users coordinates vectors constitute the training data input of the SVM-based classifier in the classification learner built-in function in MATLAB. Thereby, the trained model is created, and a theoretical accuracy of the system model is evaluated at the end of this phase. This model is used in the second phase to classify new data and test the performance of the system.



Figure 3 - The training phase.

The block diagram of the prediction phase is shown in **Error! Reference source not found.**. This phase allows to predict the belonging zone of a user and to evaluate the performance and accuracy of the model. A user location is randomly generated in the area of interest. The received signals at the array elements are then calculated. A vector S_u of length $N \times N$ is obtained. The trained model is used to predict the location zone of the user based on the signal vector.

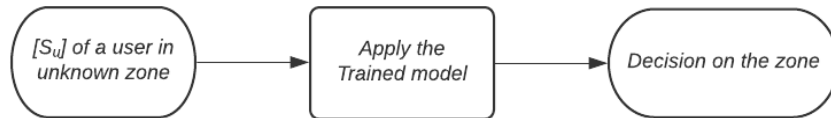


Figure 4 - The prediction phase.

CONSIDERED SCENARIOS & RESULTS

A. Introduction

We study and analyze in this section the performance, reliability, and robustness of the proposed system. We consider a cell of size $500 \times 500 \text{ m}^2$ and a BS of height $H = 30 \text{ m}$. The frequency of operation is $f = 30 \text{ GHz}$, but the analysis is performed as function of the wavelength, and the same method and analysis stay valid for other operating frequencies.

The results that will be presented show two types of accuracy: the theoretical accuracy obtained at the end of the training phase and the prediction accuracy obtained at the end of the prediction phase. The testing samples used in the prediction phase are divided into two sets, each of which of 10,000 users randomly distributed in the cell. The prediction accuracy is the average of the accuracy obtained from each of these two sets.

We perform the analysis for the case where the direct path is only received, and for the case where multipaths are present. In both cases, we study the robustness of the system in the presence of noise. Furthermore, we analyze the system performance and the effect of changing the configuration parameters. Hence, we compare the results obtained by changing: the number of training samples, the spacing between the array elements, the number of zones, and the number of array elements. At the end of this section, we show the distribution of the positions of the wrongly-predicted users and confirm that the majority of the positions of these users are close to the predicted cell.

B. Direct path performance analysis

In this part, we consider the case where the received signal corresponds only to the direct path between the user and the array. In each of the configurations we are considering, we take two values of the number of training samples in each zone: $T_z = 50$ and $T_z = 500$ samples per zone.

We compare the accuracy of the system for three values of the inter-element array spacing d : $\frac{\lambda}{4}$, $\frac{\lambda}{2}$, and $\frac{3\lambda}{4}$ respectively. We note that the optimal inter-element spacing of an antenna array to achieve high de-correlation between the signals at the different elements of the array is around $\frac{\lambda}{2}$ (Hidayah et al., 2017). We set the number of zones to 3×3 and the number of array elements to 8×8 for this comparison. We show in **Error! Reference source not found.** the theoretical and prediction accuracy for these configurations. Overall, the accuracy values increase with the increase of the number of samples per zone for all the cases. Moreover, we can see that the spacings $d = \frac{\lambda}{4}$ and $d = \frac{\lambda}{2}$ give close results, and the accuracy values in these cases are higher compared to the case where $d = \frac{3\lambda}{4}$.

Then, we set the inter-element array spacing value to $d = \frac{\lambda}{2}$ and the number of array elements to 8×8 and we compare the accuracy on the position estimation for $M \times M = 3 \times 3, 4 \times 4$, and 8×8 . For this case, we can note that the theoretical and the prediction accuracy values both increase also with the increase of the number of samples per zone. In general, when the number of zones increases, the accuracy of the system is expected to decrease due to the increment of the number of zones to be decoded. We note from **Error! Reference source not found.-a** that the accuracy values of the considered configurations for $T_z = 500$ differ by no more than 3%. Overall, we can conclude that the accuracy of our system is high, even when the width of the zones decreases.

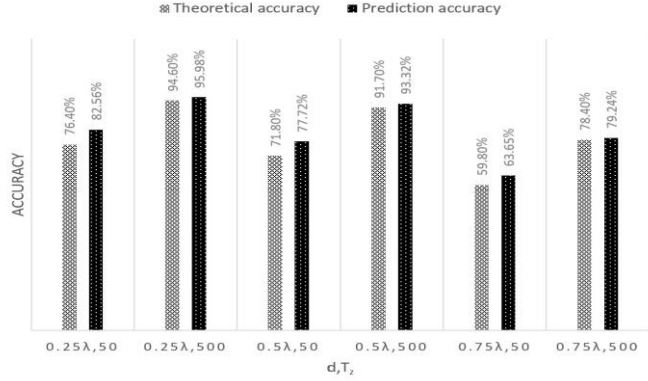
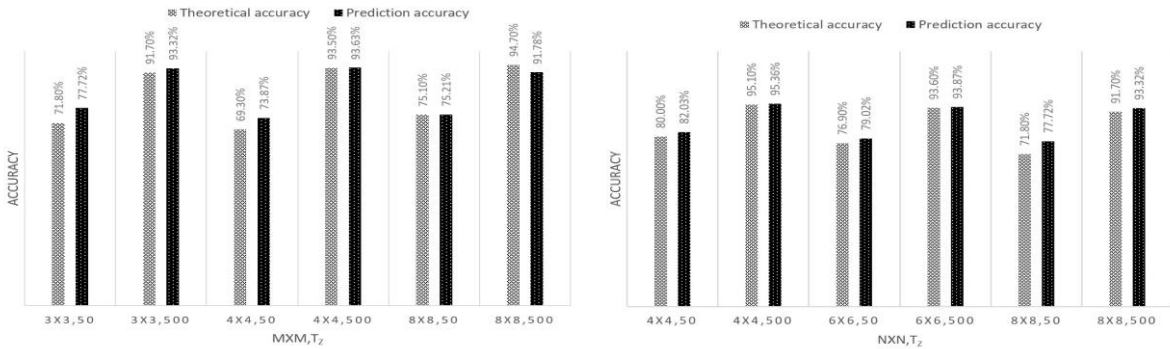


Figure 5 Model accuracy for different values of d and T_z , and for $M \times M = 3 \times 3$ and $N \times N = 8 \times 8$.



a) Impact of $M \times M$ and T_z for $N \times N = 8 \times 8$. b) Impact $N \times N$ and T_z for $M \times M = 3 \times 3$.

Figure 6 Model accuracy for different parameters by fixing $d = \frac{\lambda}{2}$.

Now we evaluate the effect of changing the number of array elements on the system performance. We compare the accuracy of the system for $N \times N = 4 \times 4$, 6×6 , and 8×8 . We set $d = \frac{\lambda}{2}$ and $M \times M = 3 \times 3$. Referring to **Error! Reference source not found.-b**, we notice as previously, the higher the number of training samples the higher the accuracy. If we take the case of $T_z = 500$ training samples per zone, the accuracy values obtained for the three considered array sizes are close and the difference does not exceed 1.5%. Changing the number of array elements will have a clearer impact in the presence of noise and multipaths scenario, that will be studied in the next parts.

C. System performance in an AWGN channel

In this part, we add to the received signal a white Gaussian noise in the testing phase of the model and we evaluate the accuracy of prediction for signal-to-noise ratio (SNR) values varying from -20 dB to 30 dB as 3GPP simulation results are often done in this range with a more focus on the range between 0 and 30 dB. We fix the number of zones to $M \times M = 3 \times 3$, and we explore the impact of varying the number of array elements ($N \times N = 4 \times 4$, 6×6 , and 8×8)

on the system accuracy for two different inter-element array spacings: $d = \frac{\lambda}{4}$ (**Error! Reference source not found.-a**) and $d = \frac{\lambda}{2}$ (**Error! Reference source not found.-b**). The number of training samples T_z in each zone is set to 500 samples per zone.

In the Wideband fifth-generation (5G) systems utilizing high carrier frequency and MIMO, the SNR requirements for extreme data rates are challenging. In fact, when we increase the modulation scheme order, the required SNR to satisfy the demand also increases. The required SNR for a given modulation is regularly set for symbol error rate to float around 10^{-3} . One of the main solutions to decrease the required SNR is to decrease the coding rate. However, the amount of transmitted data will be lower. At this stage, some tradeoffs should be taken for realistic implementation. In Tuovinen et al. (2017), the minimum required SNR for QPSK modulation schemes and higher for a decent coding rate is around 10 dB. We will refer to this specific value of SNR in our upcoming analysis.

From **Error! Reference source not found.-a** and **Error! Reference source not found.-b**, we can note that for low SNR and for any number of array elements the system performs badly and the classification corresponds to a random classification with accuracy equals to $\frac{1}{M \times M} = \frac{1}{9} = 11.11\%$. However, when the SNR increases ($-10dB \leq SNR \leq +10dB$), we can remark that for a higher number of array elements, the system can detect the DoA more accurately for both inter-element array spacing $d = \frac{\lambda}{4}$ and $\frac{\lambda}{2}$. For instance, when the SNR is 10 dB, the accuracy values for $N \times N = 4 \times 4$, 6×6 , and 8×8 are 85.60%, 89.79%, and 90.86% respectively for $d = \frac{\lambda}{2}$, and 83.47%, 89.59%, and 92.30% respectively for $d = \frac{\lambda}{4}$. Moreover, we can see that for higher SNR values (above 10 dB), the system starts to converge and gives accuracy values close to noise-free conditions. These results show the gain in SNR when increasing the number of array elements: for $d = \frac{\lambda}{2}$ and a very high accuracy of 80% (Kranjcic et al., 2019), the gain in SNR is 5 dB when the size of the array increases from 4×4 to 6×6 elements and 3 dB when it increases from 6×6 to 8×8 elements. By comparing our result to the state of the art, we can say that in our proposed method we are avoiding the complexity of MUSIC and ESPRIT (Randazzo et al., 2007). SVMs are very popular for their mathematical formulation and unbeatable robustness. After a training phase done offline, the model performs well in response to input signals that have been seen for the first time.

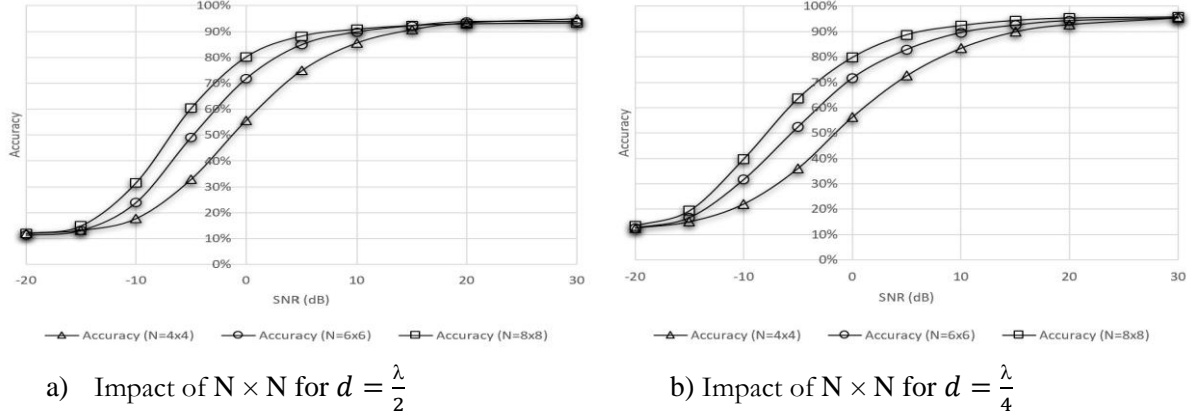


Figure 7 Model accuracy in AWGN channel for different values of $N \times N$ and d for $M \times M = 3 \times 3$.

D. System performance in multipath propagation

In this part we examine the performance of the developed system in a multipath propagation medium. We assume that the propagation medium between the user and the array has four main different multipath components (MPCs) randomly chosen between the transmitter and the receiver and is time-invariant. The received signal is thus calculated using Equation 4 for $K = 4$. Without lack of generality, the reflection points are considered isotropic and the corresponding attenuation factors can be written as $\alpha_{ij}^k = 1/(r_u^k \cdot r_{ij}^k)$, where r_u^k and r_{ij}^k are the distances between user and reflection point k , and between array element (i, j) and reflection point k , respectively. The delay τ_{ij}^k corresponds to the delay of propagation in free space for a total distance of $r_u^k + r_{ij}^k$.

This model of propagation medium is used in both the training phase and the prediction phase. We add a white Gaussian signal to the received signals in the prediction phase, vary the SNR from -20 to +30 dB, and analyze the system performance. Here, we consider the same configuration as in the previous part: the number of zones is fixed at 3×3 , the number of array elements takes the values of 4×4 , 6×6 , and 8×8 elements, d values are $\frac{\lambda}{4}$ and $\frac{\lambda}{2}$, and T_z is 500 samples per zone.

We can note, referring to **Error! Reference source not found.** and for all combinations of array elements, an inter-element array spacing of $d = \frac{\lambda}{2}$ gives higher accuracy. Also, for a larger number of array elements, the system performance is improved, but the maximum accuracy values achieved are relatively low compared to the previous results. However, the accuracy is considered as high (greater than 60%) (Kranjcic et al., 2019) for SNR greater than 10 dB and 8×8 elements. A deeper analysis of these results is done in the coming part.

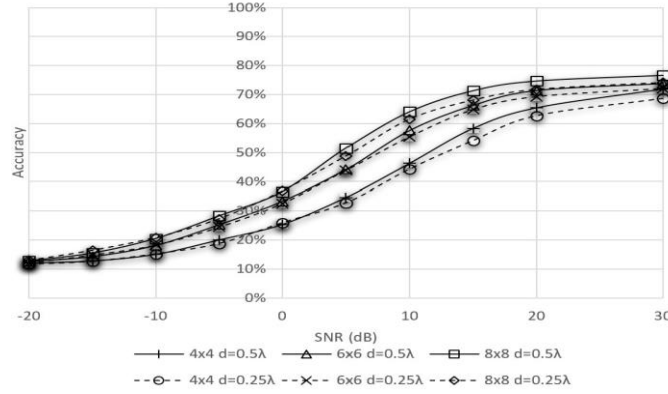


Figure 8 Model accuracy in presence of MPC for different values of $N \times N$ and d , for $M \times M = 3 \times 3$.

E. Misclassification analysis

Due to the relatively low accuracy achieved for the case of a propagation channel with MPCs compared to an AWGN channel, we propose to investigate the spatial distribution of the wrongly-predicted users. We calculate the distance, denoted D_e , between the real position of the user and the closest point in the predicted zone. A low value of D_e indicates that the error occurs for users that are close to the zone border.

In the histogram shown in **Error! Reference source not found.**, we consider the two cases studied in the previous parts: the first one corresponds to an AWGN channel, and the second one corresponds to the channel with MPCs. The SNR being set to 10 dB, the number of array elements is set to 8×8 and $d = \frac{\lambda}{2}$. We illustrate the distribution of users for $D_e = 0, 20, 40, 60$, and greater than 60 m, $D_e = 0$ indicates a correct prediction of user.

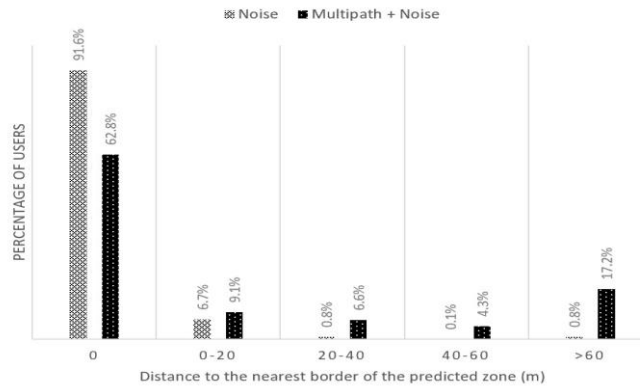


Figure 9 Spatial distribution of the predicted users in a noisy channel only and in a noisy channel with MPC at SNR=10 dB for $d = \frac{\lambda}{2}$ for $M \times M = 3 \times 3$, and $N \times N = 8 \times 8$.

Overall, we can see that the percentage of users correctly predicted is the highest for both cases. In the first case, 91.6% of users are correctly classified, and in the second case, 62.8% of users are correctly classified. The percentage of wrongly predicted users decreases with the increase of D_e for the case of an AWGN channel and is less than 1% for $D_e > 60m$, which confirms that the majority of these users are located close to the borders of the predicted zone. In the case where MPCs are considered, the percentage of the wrongly predicted users is higher than that obtained in the first case, and in particular, 17% of the users are located at least at 60 m from the border of the predicted zone. This indicates that users relatively far from the border of the predicted zone are not correctly classified, thus, the performance of the system has decreased in the case where MPCs are present.

At the end of this part, we study the effect of varying the number of array elements $N \times N$ and the inter-element array spacing d on the average of the distance D_e , for the channel with MPCs. The average is taken over the wrongly predicted users of the considered testing sample set. The SNR is set at 10 dB and the number of zones is fixed at 3×3 (**Error! Reference source not found.**). We can note, for all configurations, that the average of D_e is slightly higher for $d = \frac{\lambda}{4}$ than $d = \frac{\lambda}{2}$. Furthermore, we can confirm that when the number of array elements increases, the average D_e decreases indicating an improvement in the system performance. This average decreases to 72 m, which indicates that most of the misclassification corresponds to users located in the closest half of the adjacent zone to the predicted zone.

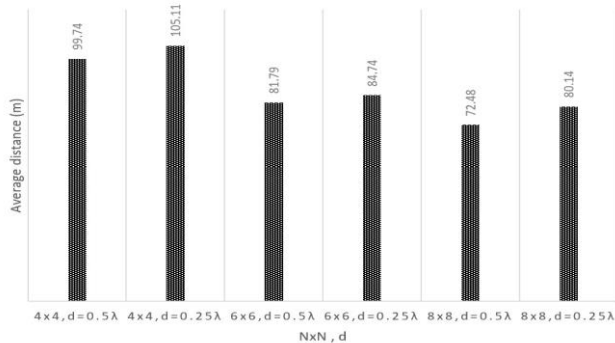


Figure 10 Average distance from the wrongly predicted users to the correct zone for different values of $N \times N$ and d in an AWGN channel with MPC at SNR=10 dB and $M \times M = 3 \times 3$.

CONCLUSION AND FUTURE WORK

In this paper, we have examined the problem of DoA estimation. The main motivation of this study is, first, the non-efficiency in radiating the main lobe of an antenna in one static direction without taking into account the distribution and the density of the users within a specific cell, and second, the increase in data rate demand, the limited bandwidth available, and the need to

introduce in the telecom networks more intelligent and dynamic algorithms to increase the efficiency of these systems.

We have developed a machine learning-based approach using SVM technique that allows to analyze a large amount of data and classify it by finding specific patterns. Different simulation results, performance analyses, and tests are presented. We have studied the performance of the whole system in the presence of white Gaussian noise and multipaths. We prove through the different simulations that the proposed system is reliable and has good performance in the presence of noise. The analysis of the system in the presence of multipaths was essential for the evaluation of its robustness in real case scenarios. We have shown that increasing the number of elements increases the accuracy of the system in presence of noise and multipaths, and that an inter-element spacing of half a wavelength is an optimum configuration.

Further research could be done in the context of this work. The proposed model has shown its applicability to localize a user in a cell for 5G emerging bands without lack of generality on the other bands. The performance of this whole system should be studied for the case of a time-varying channel. Furthermore, 5G indoor networks offer new experiences for consumers, industrial automation, high operational efficiency with IoT, and massive communication services. Multiple challenges are faced in indoor applications, and beamforming associated with DoA estimation consists of a suitable technique to face these challenges.

REFERENCES

- Yarrabothu, R.S. & Mohan, J. 2015.** A survey paper on 5g cellular technologies - technical & social challenges. *International Journal of Emerging Trends in Electrical and Electronics*. **11**(2): 98–100.
- Chin, W.H., Fan Z., & Haines R. 2014.** Emerging technologies and research challenges for 5g wireless networks. *IEEE Wireless Communications*. **21**(2):106–112.
- Niu, Y.L.Y., Jin, L.S.D., & Vasilakos, A.V. 2015.** A survey of millimeter wave communications (mmwave) for 5g: opportunities and challenges. *Wireless Networks*: 2657–2676.
- Heath, R.W., González-Prelcic, N., Rangan, S., Roh, W., & Sayeed, A.M. 2016.** An overview of signal processing techniques for millimeter wave mimo systems. *IEEE Journal of Selected Topics in Signal Processing*. **10**(3): 436–453.
- Al-Falahy, N. & Alani, O. 2019.** Millimetre wave frequency band as a candidate spectrum for 5g network architecture: A survey. *Physical Communication*. **12**: 120–144.

Cella, T., Orten, P., & Ekman, T. 2014. Design of a practical and compact mm-wave mimo system with optimized capacity and phased arrays. *International Journal of Antennas and Propagation*. 2014

Rappaport, T.S., Xing, Y., MacCartney, G.R., Molisch, A.F., Mellios, E.E., & Zhang, J. 2017. Overview of millimeter wave communications for fifth-generation (5g) wireless networks—with a focus on propagation models. *IEEE Transactions on Antennas and Propagation*. **65**(12): 6213–6230.

Liang, Y.C., Chen, K.C., Li, G.Y., & Mähönen, P. 2011. Cognitive radio networking and communications: an overview. *IEEE Transactions on Vehicular Technology*. **60**(7): 3386–3407.

Liu, X., He, D., & Jia, M. 2017. 5g-based wideband cognitive radio system design with cooperative spectrum sensing. *Physical Communication*. **25**(2): 539–545.

Bogale, T.E. & Le, L.B. 2016. Massive mimo and mmwave for 5g wireless hetnet: potential benefits and challenges. *IEEE Vehicular Technology Magazine*. **11**(1): 64–75.

Bshara, Y.L.O., Tekin, I., Taskin, B., & Dandekar, K.R. 2018. mm wave antenna gain switching to mitigate indoor blockage. *IEEE International Symposium on Antennas and Propagation & USNC/URSI National Radio Science Meeting*.

Schmidt, R. 1986. Multiple emitter location and signal parameter estimation. *IEEE Transactions on Antennas and Propagation*. **34**(3): 276-280.

Roy, R., & Kailath, T. 1989. ESPRIT-Estimation of signal parameters via rotational invariance techniques. *IEEE Trans. Acoust., Speech, Signal Process*. **37**: 984-995.

El Zooghby, A.H., Christodoulou, C.G., & Geogiopoulos, M. 1997. Performance of radial-basis function network for direction arrival estimation with antenna arrays. *IEEE Trans. Antennas Propag.* **45**: 1611-1617.

El Zooghby, A.H., Christodoulou, C.G., & Geogiopoulos, M. 2000. A neural network-based smart antenna for multiple source tracking. *IEEE Trans. Antennas Propag.* **45**: 768-776.

Randazzo, M.A.A., Pastorino, M., & Zoughi, R. 2007. Direction of Arrival Estimation Based on Support Vector Regression: Experimental Validation and Comparison With MUSIC. *IEEE Antennas and Wireless Propagation Letters*. **6**: (379-382).

Cortes, C. & Vapnik, V. 1995. Support-vector networks. *Machine Learning*. **20**: 273–297.

Ladicky, L. & Torr, P. 2011. Locally linear support vector machines. *Proceedings of the 28th International Conference on Machine Learning*.

- Suykens, J.A.K. 2001.** Nonlinear modelling and support vector machines. Instrumentation and Measurement Technology Conference. **1**: 287–294.
- Awad, M. & Khanna, R. 2015.** Support vector machines for classification. Efficient Learning Machines: Theories, Concepts, and Applications for Engineers and System Designers: 39–66.
- Wang, Y., Zhang, Z., Ma, L., & Chen, J. 2014.** Svm-based spectrum mobility prediction scheme in mobile cognitive radio networks. The Scientific World Journal. **2014**
- Zhao, X., Hou, C., & Wang, Q. 2013.** A new svm-based modeling method of cabin path loss prediction. International Journal of Antennas and Propagation. **2013**.
- Uccellari, M., Facchini, F., Sola, M., Sirignano, E., Vitetta, G.M., Barbieri, A., & Tondelli, S. 2018.** On the application of support vector machines to the prediction of propagation losses at 169 mhz for smart metering applications. IET Microwaves, Antennas and Propagation. **12**(3): 302–312.
- Zhang, Y., Yang, J.G., He, Z., & Wang, J. 2019-1.** Path loss prediction based on machine learning: principle, method, and data expansion. Applied Sciences. **9**(9): 302–312.
- Feng, B., Yi, L., Xu, L., Jiang, H., & Ruan, Y. 2013.** Abnormal signal recognition of fm broadcast band based on support vector machine. ICIC Express Letters. **7**: 3213–3220.
- Xu, J., Ying, S., & Li, H. 2020.** Gps interference signal recognition based on machine learning,” Mobile Networks and Applications.
- Sun, F., Tian, Y., Hu, G., & Shen, Q. 2019.** DoA estimation based on support vector machine ensemble. International Journal of Numerical Modelling: Electronic Networks, Devices and Fields. **32**(5).
- Zhang, J., Wang, Q., Yang, L., & Feng, T. 2019-2.** Formal verification of 5g-eap-tls authentication protocol. IEEE Fourth International Conference on Data Science in Cyberspace (DSC).
- Rappaport, T.S. 2001.** Wireless communications: principles and practice. Prentice Hall, Second edition.
- Godara, L.C. 2002.** Handbook of antennas in wireless communications. CRC Press LLC Inc., First edition.
- Hidayah, N., Adnan, M., Rafiqul, I., & Alam A. 2017.** Effects of inter element spacing on large antenna array characteristics. Proc. of the 4th IEEE International Conference on Smart Instrumentation, Measurement and Applications (ICSIMA).

Tuovinen, T., Tervo, N., & Pärssinen, A. 2017. Analyzing 5g rf system performance and relation to link budget for directive mimo. *IEEE Transactions on Antennas and Propagation*. **65**(12): 6636–6645.

Kranjic, N., Medak, M., Župan, R., & Rezo, M. 2019. Support Vector Machine Accuracy Assessment for Extracting Green Urban Areas in Towns. *Remote Sensing*. **11**(6): 655-667.